Biointerface Research in Applied Chemistry
Platinum Open Access Journal (ISSN: 2069-5837)

Article
Volume 11, Issue 6, 2020, 14580 - 14590
https://doi.org/10.33263/BRIAC116.1458014590

Preparation of Supramolecular Material from Amylosic Inclusion Complex with Thermoresponsive Guest Polymer Obtained by Vine-Twining Polymerization

Jun-Ichi Kadokawa [1,*], Keisuke Yano [1], Kazuya Yamamoto [1]

[1] Graduate School of Science and Engineering, Kagoshima University, 1-21-40 Korimoto, Kagoshima 890-0065, Japan
* Correspondence: kadokawa@eng.kagoshima-u.ac.jp;

Scopus Author ID 56261449600
Received: 11.02.2021; Revised: 4.03.2021; Accepted: 7.03.2021; Published: 25.03.2021

Abstract: Amylose constructs supramolecular inclusion complexes with polymeric guests in phosphorylase-catalyzed enzymatic polymerization field, called 'vine-twining polymerization'. However, such inclusion complexes have not exhibited specific property and processability as functional supramolecular materials. In a recent study, n amphiphilic triblock guest copolymer (poly(2-methyl-2-oxazoline-*block*-tetrahydrofuran-*block*-2-methyl-2-oxazoline, (P(MeOx-*block*-THF-*block*-MeOx)) was employed for the vine-twining polymerization to form soft materials from an amylosic inclusion complex. In this study, we investigated the vine-twining polymerization using a thermoresponsive triblock guest copolymer, that is, poly(2-isopropyl-2-oxazoline-*block*-tetrahydrofuran-*block*-2-isopropyl-2-oxazoline (P(iPrOx-*block*-THF-*block*-iPrOx)). The vine-twining polymerization at the temperature below the lower critical solution temperature (LCST) of PiPrOx gave the inclusion complex, while no inclusion by an enzymatically produced amylose took place at the temperature above the LCST of PiPrOx due to aggregation of P(iPrOx-*block*-THF-*block*-iPrOx) in aqueous buffer (polymerization solvent). The product's characterization results suggested that the cavity of the enzymatically elongated amylose chain included the PTHF block in the triblock copolymer by hydrophobic interaction. Accordingly, the outer PiPrOx blocks constructed spaces among the inclusion complex segments. Such higher-order structure formed supramolecular networks, leading to the formation of a hydrogel. The product showed thermoresponsive property depending upon the temperatures below and above the LCST of PiPrOx.

Keywords: amylose; inclusion complex; supramolecular material; termoresponsive polymer; vine-twining polymerization.

1. Introduction

Amylose is a well-known natural polysaccharide as a component of starch, which is recognized as a functional polymeric material because of its regularly controlled left-handed helical conformation, composed of α(1→4)-linked glucose (G) repeating units (α(1→4)-glucan) [1, 2]. Therefore, amylose has been employed as a component in functional supramolecular materials even in recent years [3, 4]. Owning to hydrophobicity inside a cavity of the amylose helix, it can bind hydrophobic guest molecules with appropriate sizes, mostly monomeric molecules, by hydrophobic interaction to form amylosic supramolecular inclusion complexes, called V-amylose [5]. Amylosic inclusion complexes with polymeric guest molecules with high molecular weights are identified to have a potential for employing in

practical applications as supramolecular materials compared to those with such monomeric guests [6, 7]. Some approaches on the direct formation of amylosic inclusion complexes from hydrophobic guest polymers have successfully been reported, as examples of the introduction of suitable hydrophilic groups at the polymer chain ends, exchange from small guest molecules to large (polymeric) ones, and the inclusion of polymerization approach [8-12]. Also, the direct mixing approach under the selected conditions has been achieved to form an inclusion complex from amylose and poly(tetrahydrofuran) (PTHF) [13-15].

We have previously reported the in-situ formation of amylose-polymer inclusion complexes in a phosphorylase-catalyzed enzymatic polymerization field [6, 7,16-26]. The enzymatic polymerization progresses by using α-D-glucose 1-phosphate (G-1-P) as a monomer, which is initiated from the chain end (non-reducing end) of a maltooligosaccharide primer (α(1→4)-linked oligoglucan) [27-34]. The propagation occurs according to the following manner in reversible reactions, i.e., $(\alpha(1\rightarrow4)\text{-G})_n$ + G-1-P ⇄ $(\alpha(1\rightarrow4)\text{-G})_{n+1}$ + Pi (inorganic phosphate). By dispersing guest polymers with moderate hydrophobicity in the aqueous enzymatic polymerization system, the propagation progresses with including the guest polymers in the cavity, giving rise to amylose-polymer inclusion complexes. Because the sufficient dynamic field for the more efficient complexation with polymeric guests than the direct complexation is provided during the phosphorylase-catalyzed enzymatic chain-elongation from the short maltooligosaccharide primer to the longer amylose, we have proposed that this polymerization method can be named "vine-twining polymerization" for the formation of amylose-polymer inclusion complexes, where the representation of this system is similar to plant vines twining around a rod.

Although various hydrophobic polymers have been found to be used as guests in the vine-twining polymerization, like hydrophobic polyethers (e.g., PTHF), polyesters, and polycarbonates [35-40], all the resulting inclusion complexes, regardless of guest polymers, have shown powdery appearances and not exhibited specific property and processability as functional supramolecular materials, such as soft material formation, probably due to regular crystalline structure and insufficient mechanical property of V-amylose. In the previous study, we reported successfully fabricate amylosic supramolecular soft materials, such as film and gel, from the vine-twining polymerization products by employing a triblock copolymer comprising an inner hydrophobic PTHF block and outer hydrophilic poly(2-methyl-2-oxazoline) (PMeOx) blocks (P(MeOx-block-THF-block-MeOx)) with amphiphilic property [41]. The product constructed a new higher-order structure because the outer PMeOx chains formed hydrophilic spaces among inclusion complex (V-amylose) segments with the inner PTHF chain and lower regularity of crystalline alignment among the V-amylose segments that was suitable for the production of the soft supramolecular material.

In this study, we employed another triblock copolymer as a new guest polymer, which is comprising an inner PTHF block and outer poly(2-isopropyl-2-oxazoline) (PiPrOx) blocks (P(iPrOx-block-THF-block-iPrOx)), for the vine-twining polymerization to produce an amylosic inclusion complex with unique functions (Figure 1). The poly(2-alkyl-2-oxazoline) properties have been known to adjust by altering the alkyl substituents at position 2 on the oxazoline rings; for example, the lengths of carbon chains in the substituents determine the hydrophilic/hydrophobic properties of the poly(2-alkyl-2-oxazoline)s [42-49]. Interestingly, PiPrOx exhibited thermoresponsive property with the lower critical solution temperature (LCST) of ca. 38 ºC [50, 51]. Therefore, P(iPrOx-block-THF-block-iPrOx) also shows the thermoresponsive property, in which its hydrophilic property at lower temperature turns into

hydrophobicity by elevating temperature. Consequently, the present amylosic inclusion complex with P(iPrOx-block-THF-block-iPrOx), formed by the vine-twining polymerization, was found to show different behaviors responded by temperatures in addition to the hydrogel formation.

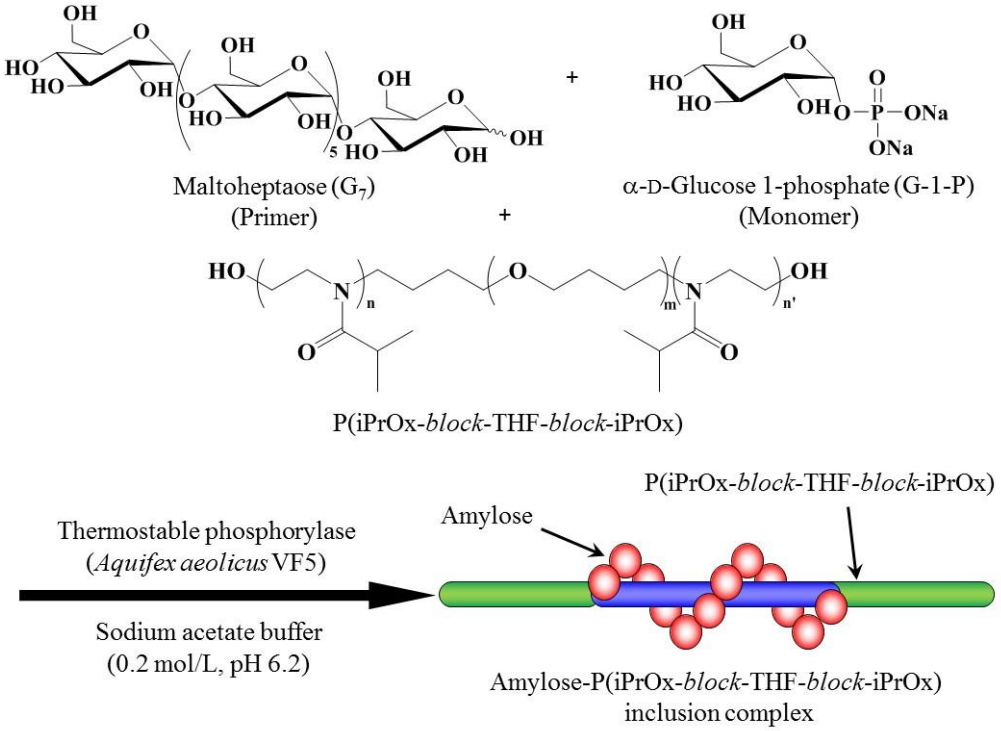

Figure 1. Vine-twining polymerization using P(iPrOx-*block*-THF-*block*-iPrOx) as guest polymer.

2. Materials and Methods

2.1. Materials.

iPrOx was prepared from isobutyronitrile and 2-aminoethanol in the presence of zinc acetate according to the literature procedure and purified by distillation [52]. Trifluoromethanesulfonic anhydride (Tf_2O) was prepared from trifluoromethanesulfonic acid by treatment with phosphorus pentoxide and distilled for purification. PTHF was prepared by ring-opening polymerization of THF initiated with ethyl trifluoromethanesulfonate (EtOTf) according to the literature procedure [53]. Thermostable phosphorylase (*Aquifex aeolicus* VF5) was kindly provided by Ezaki Glico Co. Ltd., Osaka, Japan [54, 55].

2.2. Synthesis of P(iPrOx-block-THF-block-iPrOx .

A mixture of THF (1.76 mL, 20.0 mmol) and Tf_2O (0.169 mL, 1.0 mmol) was stirred at 0 °C for 15 min under argon. After iPrOx (2.98 mL, 50.0 mmol) was added to the resulting solution at -78 °C, the mixture was successively stirred at that temperature for 1 h, left standing at room temperature for 30 min, and stirred at 60°C for 24 h. The propagating end was deactivated by the addition of sat. $NaHCO_3$ aq. (5.0 mL) to the solution. After the mixture was evaporated, methanol (100 mL) was added, and inorganic salts were filtered off. After the filtrate was evaporated and methanol (5.0 mL) was added, the solution was poured into hexane (150 mL)/diethyl ether (100 mL) mixture for the precipitation of the product. The precipitate was separated by centrifugation and dried under reduced pressure to obtain P(iPrOx-block-

THF-block-iPrOx) (2.70 g). ^{1}H NMR (CD_3OD) δ 1.05 (br, -CH_3 of PiPrOx), 1.57 (br, -C-CH_2CH_2-C- of PTHF), 2.71-2.98 (br, -CH- of PiPrOx), 3.23-3.59 (br, -CH_2O- of PTHF, -CH_2N- of PiPrOx).

A mixture of the resulting copolymer (0.10 g) and acetic anhydride (3.0 mL) in pyridine (3.0 mL) was maintained at room temperature overnight with stirring. The resulting mixture was then poured into hexane (100 mL) to obtain the precipitate, which was separated by centrifugation and dried under reduced pressure to yield the acetyl-terminated triblock copolymer (71.4 mg). ^{1}H NMR (CD_3OD) δ 4.20-4.24 (br, -CH_2O(C=O)CH_3 (terminal acetate methylene)). From the integrated ratio of this signal to a methylene signal of PTHF block (-C-CH_2CH_2-C-) at δ 1.57 and a methyl signal of PiPrOx block at δ 1.05, the values of M_n of the triblock copolymer and degrees of polymerization (DPs) of PTHF and PiPrOx blocks were calculated to be 8090, 25.5, and 53.2.

2.3. Vine-twining polymerization.

Ultrasonication of a mixture of G-1-P (0.152 g, 0.50 mmol), G_7 (5.8 mg, 5.0 μmol), and P(iPrOx-*block*-THF-*block*-iPrOx) (0.256 g, 0.10 mmol) in sodium acetate buffer (pH = 6.2, 0.2 mol/L, 7.5 mL) was first performed for 2 h to obtain a dispersion. After the addition of thermostable phosphorylase (90 U) to the dispersion, the mixture was maintained at 30 °C for 24 h with stirring. The precipitate was then isolated by filtration, washed with water and methanol, and dried under reduced pressure to obtain the inclusion complex (56.5 mg). ^{1}H NMR (DMSO-d_6) δ 0.97 (br, -CH_3 of PiPrOx), 1.50 (br, -C-CH_2CH_2-C- of PTHF), 2.62-2.86 (br, -CH of PiPrOx), 3.25-3.65 (m, -CH_2O- of PTHF, -CH_2N- of PMeOx, H2-H6 of amylose, overlapping with HOD), 5.10 (br, H1), 4.60, 5.43, 5.54 (OH of amylose).

2.4. Formation of the hydrogel.

After a mixture of the inclusion complex (25.0 mg) with methanol (30 mL) was ultrasonicated for 2 h and centrifugated, the supernatant was decantated off. The paste-like swollen material was immersed in water (30 mL) for 24 h to obtain the hydrogel. The hydrogel was left standing at room temperature or 50 °C overnight and then immediately lyophilized to give cryogels. The water content was calculated by the weight difference between the hydrogel and its lyophilized sample.

2.5. Measurements.

^{1}H NMR spectra were recorded on JEOL ECA600 spectrometer. Powder X-ray diffraction (XRD) measurements were conducted using a PANalytical X'Pert Pro MPD diffractometer with Ni-filtered Cu Kα radiation (λ = 0.15418 nm). Scanning electron microscopic (SEM) images were obtained using a Hitachi S-4100H electron microscope.

3. Results and Discussion

The triblock guest copolymer (P(iPrOx-block-THF-block-iPrOx)) was synthesized by ring-opening block copolymerization of THF with iPrOx initiated by Tf_2O according to the literature procedure [56]. After acetylation of terminal hydroxy groups were conducted using acetic anhydride in pyridine, the M_n value of the triblock copolymer and the DP values of the PTHF and PiPrOx blocks were estimated by integrated ratios of a methylene signal (-C-

CH_2CH_2-C-) of the PTHF blocks and a methyl signal of the PiPrOx blocks to a methylene signal of the terminal acetate groups (-$CH_2O(C=O)CH_3$) in the ^{1}H NMR spectrum of the products in CD_3OD to be 8090, 25.5, and 53.2. A homopolymer (PTHF) for a contrast experiment was also prepared by ring-opening polymerization of THF initiated by EtOTf [53].

The vine-twining polymerization using the synthesized P(iPrOx-block-THF-block-iPrOx) as the guest polymer was then carried out in the enzymatic polymerization of G-1-P (5 equiv. with the guest polymer) in the presence of G_7 (1/100 equiv. with G-1-P) catalyzed by phosphorylase in 0.2 mol/L sodium acetate buffer (pH 6.2) under dispersion condition of the guest polymer at temperatures below (30 °C) and above (50 °C) the LCST of PiPrOx (38 °C) (Figure 1). The mixtures were stirred at the desired temperatures for 24 h, and the resulting precipitates were then separated by filtration and washed with water and methanol to give the products.

The products thus obtained by the vine-twining polymerization were characterized by XRD and ^{1}H NMR measurements. The XRD profile of the product obtained at 30 °C show two typical diffraction peaks at around 20 and 13° assignable to the helical pitch in the inclusion complex and the distance between the helix centers (corresponding to approximately a diameter) (Figure 1(a)) [57], which is identical with the pattern of the inclusion complex from PTHF (Figure 1(c)) [35], but completely different from that of a pure amylose sample (Figure 1(d)). This XRD profile suggested that the inclusion complex was formed in the present system using P(iPrOx-block-THF-block-iPrOx) at the temperature below the LCST of PiPrOx.

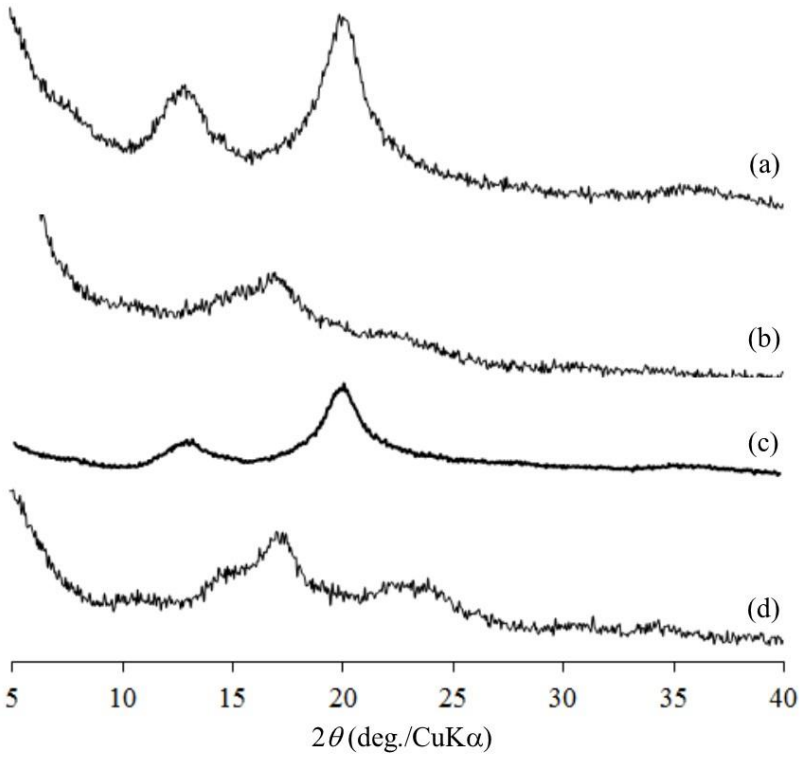

Figure 2. XRD profiles of vine-twining polymerization products obtained at (a) 30 and (b) 50 °C, (c) amylose-PTHF inclusion complex, and (d) amylose.

The ^{1}H NMR result of the product measured in DMSO-d_6 also supported the inclusion complex's formation because of the detection of both the signals assigned to amylose and the PTHF and PiPrOx protons (Figure 3(a)). The inclusion ratio of the amylose cavity to the THF block was evaluated by the integrated ratio of the H1 (anomeric) signal of the G residues to the methylene signal b (-C-CH_2CH_2-C-) of PTHF block (H1/b) in the ^{1}H NMR spectrum according

to the calculation method reported in our previous literature on the vine-twining polymerization using PTHF [37]. Generally, one helical turn of amylose comprises ca. six G units when linear and slender molecules, like PTHF, are included [58]. A repeat distance of the amylose helix and a unit length of PTHF have been calculated to be 0.80 and 0.60 nm. Accordingly, a unit length of PTHF corresponds to an average of 4.5 repeating G units in amylose. From these calculations, the integrated ratio of the H1 signal to the methylene signal (H1/b) in the ^{1}H NMR spectrum should be ideally 1.13, while the H1/b integrated value in the measured ^{1}H NMR spectrum of the vine-twining polymerization product was calculated to be 0.63 (ca. 56% of the theoretical value). This result indicated that the enzymatically elongated amylose chain preferentially included the hydrophobic PTHF block by hydrophobic interaction rather than the hydrophilic PiPrOx blocks at the temperature below the LCST. Therefore, the vine-twining polymerization product can be identified to be composed of the inner amylose-PTHF inclusion complex segment and the outer non-included PiPrOx segments, as similar to that obtained by the same operation using P(MeOx-block-THF-block-MeOx) [41].

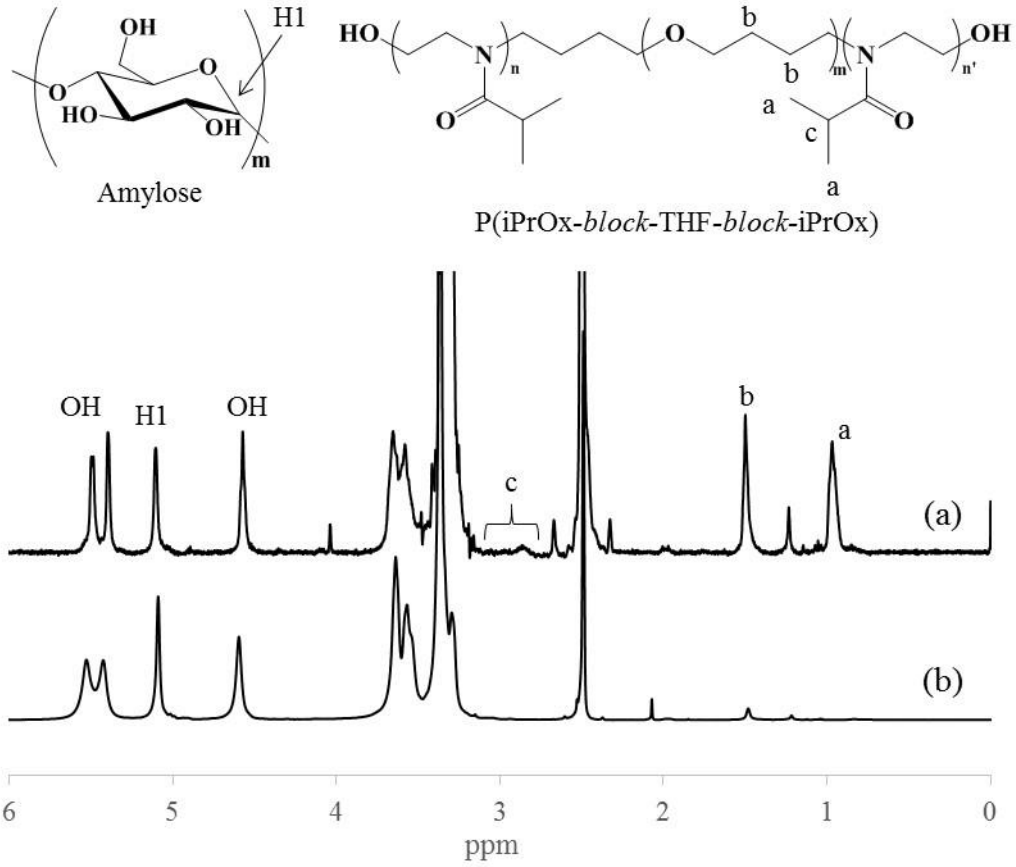

Figure 3. ^{1}H NMR spectra of vine-twining polymerization products obtained at (a) 30 and (b) 50 °C in DMSO-d_6.

The vine-twining polymerization using P(iPrOx-block-THF-block-iPrOx) was also conducted at the temperature above the LCST of PiPrOx (50 °C). The XRD and ^{1}H NMR results of the precipitated product have suggested that the enzymatically produced amylose does not include P(iPrOx-block-THF-block-iPrOx) at all at this temperature because the XRD pattern is identical with that of a pure amylose sample (Figure 2(b) and (d)) and the ^{1}H NMR spectrum detects only amylose signals (Figure 3(b)). This was attributed to the strong aggregation of P(iPrOx-block-THF-block-iPrOx) in the aqueous buffer solvent due to its entire hydrophobicity at the temperature above the LCST of PiPrOx (Figure 4(b)). At the temperature

below the LCST of PiPrOx (room temperature), on the other hand, P(iPrOx-block-THF-block-iPrOx) dispersed well in the solvent owing to its amphiphilic nature at the temperature (Figure 4(a)), leading to the formation of the inclusion complex as abovementioned.

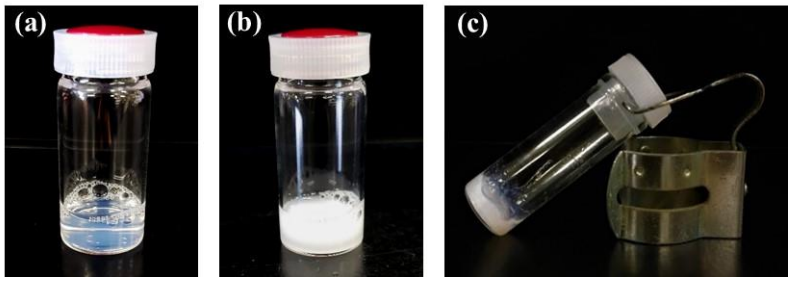

Figure 4. Photographs of mixtures of P(iPrOx-*block*-THF-*block*-iPrOx) in acetate buffers at (a) room temperature and (b) 50 ºC and (c) hydrogel formed from vine-twining polymerization product obtained at 30 ºC.

An attempt was made to form a hydrogel from the present vine-twining polymerization product by the same procedure as the previously reported material using P(MeOx-block-THF-block-MeOx) [41]. When the present product obtained at 30 ºC was treated with methanol with ultrasonication, and then the resulting paste-like material was immersed in water, the hydrogel was obtained (Figure 4(c)). The resulting hydrogel was left standing at the temperatures below and above the LCST of PiPrOx (room temperature and 50 ºC, respectively) overnight and immediately lyophilized to give the cryogels. From the weight differences between the obtained hydrogels and their lyophilized samples, the water contents after standing at room temperature and 50 ºC were calculated to be 88.9 and 71.3%, respectively. The SEM images of both the cryogels observe porous morphologies, but their pore sizes are obviously different; the sample size obtained after standing at 50 ºC is much smaller than that of the other sample (Figure 5). At the temperature above the LCST of PiPrOx, the corresponding outer blocks in the vine-twining polymerization product became hydrophobic, leading to releasing water from the hydrogel. Accordingly, the hydrogel's water content after standing at the temperature above the LCST of PiPrOx was lower and resulted in smaller pore size of the cryogel than those of the other hydrogel and cryogel.

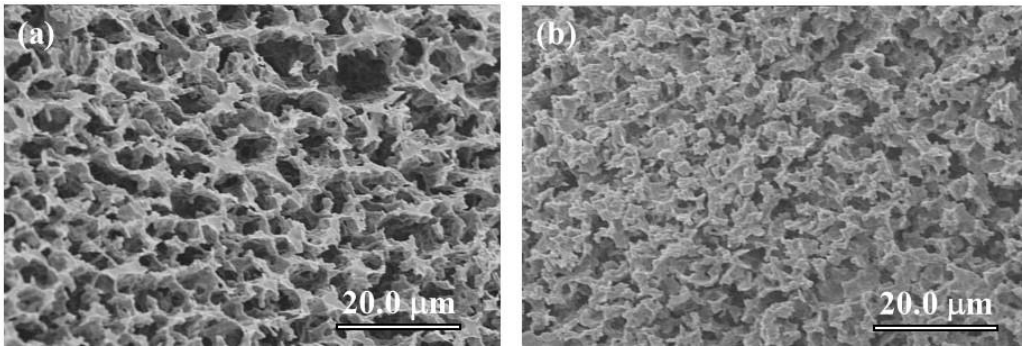

Figure 5. SEM images of cryogels obtained by lyophilization of hydrogels after standing at (a) room temperature and (b) 50 ºC.

The difference in the crystalline structures of the two cryogels after standing the hydrogels at room temperature and 50 ºC was evaluated by their XRD measurement. The area ratio of two peaks, i.e., peak A at 13º to peak B at 20º in the XRD profile of the former sample, decreases much larger than that in the XRD profile of the latter sample (0.23:1 and 0.26:1, respectively, Figure 6(b) and (c)), compared to the as-prepared vine-twining polymerization

product obtained at 30 °C (0.28:1, Figure 6(a)). As these peaks were ascribed to the distance between the helix centers in the crystalline structure among the inclusion complexes and the helical pitch of amylose helix in the inclusion complex, respectively [57], the XRD results suggested that regularity of the crystalline alignment among the complexes (V-amylose) was lowered by treatment of the hydrogel at room temperature more than that at 50 °C. As suggested in the previous study [41], the hydrogenation in the present system was considered to be similarly achieved by the formation of network structures from the vine-twining polymerization product of amylose with P(iPrOx-block-THF-block-iPrOx), which were composed of cross-linking points constructed by the crystalline alignments among the inner amylose-PTHF inclusion complex segments in spaces formed by the outer non-included PiPrOx blocks. Therefore, larger networks with lower regularity of the V-amylose crystalline alignment were formed by treating the hydrogel at the temperature below the LCST of PiPrOx, resulting in the higher water content and larger pore size (Figure 7(a)). On the other hand, the hydrogel treatment at the temperature above the LCST of PiPrOx constructed smaller networks with a higher regularity of the V-amylose crystalline alignment, giving rise to the lower water content and smaller pore size (Figure 7(b)).

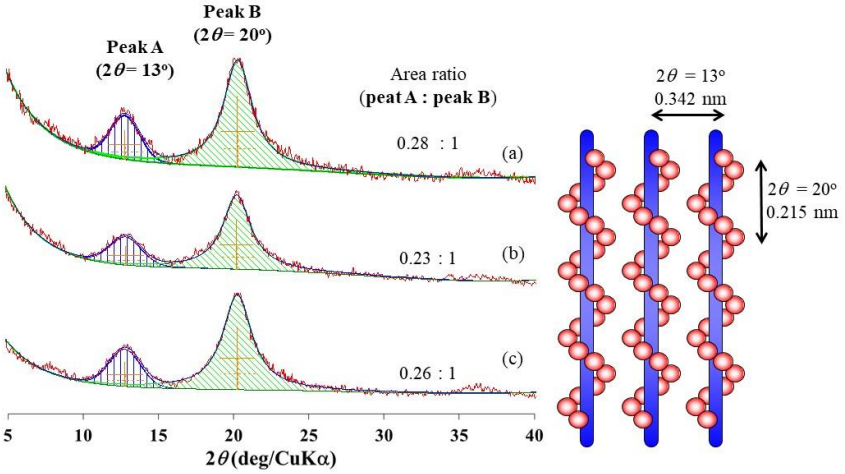

Figure 6. XRD profiles of (a) as-prepared vine-twining polymerization product obtained at 30 °C and cryogels obtained by lyophilization of hydrogels after standing at (b) room temperature and (c) 50 °C.

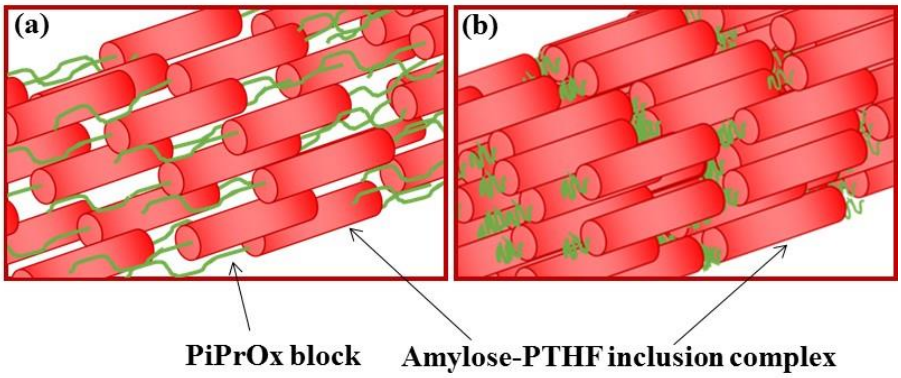

Figure 7. Plausible network structures in hydrogels after standing at (a) room temperature and (b) 50 °C.

4. Conclusions

In this study, we investigated the vine-twining polymerization using the thermoresponsive triblock guest copolymer, that is, P(iPrOx-*block*-THF-*block*-iPrOx). The vine-twining polymerization at the temperature below the LCST of PiPrOx resulted in the

formation of the inclusion complex, while no inclusion occurred at the temperature above the LCST of PiPrOx. In the vine-twining polymerization product, the amylose chain is specifically complexed with the PTHF block in the triblock copolymer to form the inclusion complex having the non-included PiPrOx chains at both sides. Consequently, the PiPrOx chains formed spaces among the amylose-PTHF inclusion complex segments. Because of such a higher-order structure, the product formed the supramolecular networks, leading to hydrogel formation. The water contents and network sizes in the products were changed depending upon the temperatures below and above the LCST of PiPrOx to treat the hydrogels. This study's resulting supramolecules can be employed as a thermoresponsive material in practical applications such as biomedical and environmentally benign fields in the future.

Funding

This research received no external funding.

Acknowledgments

The authors acknowledge the supplement of thermostable phosphorylase from Ezaki Glico Co. Ltd., Osaka, Japan.

Conflicts of Interest

The authors declare no conflict of interest.

References

1. Rostamabadi, H.; Falsafi, S.R.; Jafari, S.M. Nano-helices of amylose for encapsulation of food ingredients. In: *Biopolymer Nanostructures for Food Encapsulation Purposes*. **2019**; pp 463-491, https://doi.org/10.1016/B978-0-12-815663-6.00016-1.
2. Seung, D. Amylose in starch: towards an understanding of biosynthesis, structure and function. *New Phytol.* **2020**, *228*, 1490-1504, https://doi.org/10.1111/nph.16858.
3. Kadokawa, J. Enzymatic preparation of functional polysaccharide hydrogels by phosphorylase catalysis. *Pure Appl. Chem.* **2018**, *90*, 1045-1054, https://doi.org/10.1515/pac-2017-0802.
4. Kadokawa, J.; Egashira, N.; Yamamoto, K. Chemoenzymatic preparation of amylose-grafted chitin nanofiber network materials. *Biomacromolecules* **2018**, *19*, 3013-3019, https://doi.org/10.1021/acs.biomac.8b00577.
5. Putseys, J.A.; Lamberts, L.; Delcour, J.A. Amylose-inclusion complexes: Formation, identity and physico-chemical properties. *J. Cereal. Sci.* **2010**, *51*, 238-247, https://doi.org/10.1016/j.jcs.2010.01.011.
6. Orio, S.; Yamamoto, K.; Kadokawa, J. Preparation and material application of amylose-polymer inclusion complexes by enzymatic polymerization approach. *Polymers* **2017**, *9*, https://doi.org/10.3390/polym9120729.
7. Kadokawa, J. Synthesis of amylosic supramolecular materials by glucan phosphorylase-catalyzed enzymatic polymerization according to the vine-twining approach. *Synlett* **2020**, *31*, 648-656, https://doi.org/10.1055/s-0039-1690804.
8. Shogren, R.L.; Greene, R.V.; Wu, Y.V. Complexes of starch polysaccharides and poly(ethylene coacrylic acid) - structure and stability in solution. *J. Appl. Polym. Sci.* **1991**, *42*, 1701-1709, https://doi.org/10.1002/app.1991.070420625.
9. Shogren, R.L. Complexes of starch with telechelic poly(e-caprolactone) phosphate. *Carbohydr. Polym.* **1993**, *22*, 93-98, https://doi.org/10.1016/0144-8617(93)90071-B.
10. Star, A.; Steuerman, D.W.; Heath, J.R.; Stoddart, J.F. Starched carbon nanotubes. *Angew. Chem. Int. Ed.* **2002**, *41*, 2508-1512, https://doi.org/10.1002/1521-3773(20020715)41:14<2508::Aid-Anie2508>3.0.Co;2-A.
11. Ikeda, M.; Furusho, Y.; Okoshi, K.; Tanahara, S.; Maeda, K.; Nishino, S.; Mori, T.; Yashima, E. A luminescent poly(phenylenevinylene)-amylose composite with supramolecular liquid crystallinity. *Angew. Chem. Int. Ed.* **2006**, *45*, 6491-6495, https://doi.org/10.1002/anie.200602134.
12. Kumar, K.; Woortman, A.J.J.; Loos, K. Synthesis of amylose-polystyrene inclusion complexes by a facile preparation route. *Biomacromolecules* **2013**, *14*, 1955-1960, https://doi.org/10.1021/Bm400340k.

13. Rachmawati, R.; Woortman, A.J.J.; Loos, K. Facile preparation method for inclusion complexes between amylose and polytetrahydrofurans. *Biomacromolecules* **2013**, *14*, 575-583, https://doi.org/10.1021/Bm301994u.
14. Rachmawati, R.; Woortman, A.J.J.; Loos, K. Tunable properties of inclusion complexes between amylose and polytetrahydrofuran. *Macromol. Biosci.* **2013**, *13*, 767-776, https://doi.org/10.1002/mabi.201300022.
15. Rachmawati, R.; Woortman, A.J.J.; Loos, K. Solvent-responsive behavior of inclusion complexes between amylose and polytetrahydrofuran. *Macromol. Biosci.* **2014**, *14*, 56-68, https://doi.org/10.1002/mabi.201300174.
16. Kaneko, Y.; Kadokawa, J. Vine-twining polymerization: A new preparation method for well-defined supramolecules composed of amylose and synthetic polymers. *Chem. Rec.* **2005**, *5*, 36-46, https://doi.org/10.1002/Tcr.20031.
17. Kaneko, Y.; Kadokawa, J. Synthesis of nanostructured bio-related materials by hybridization of synthetic polymers with polysaccharides or saccharide residues. *J. Biomater. Sci., Polym. Ed.* **2006**, *17*, 1269-1284, https://doi.org/10.1163/156856206778667479.
18. Kaneko, Y.; Kadokawa, J. Preparation of polymers with well-defined nanostructure in the polymerization field. In: *Modern Trends in Macromolecular Chemistry*. Lee, J.N. Ed. Nova Science Publishers, Inc.: Hauppauge, NY, **2009**; pp 199-217.
19. Kadokawa, J. Preparation and applications of amylose supramolecules by means of phosphorylase-catalyzed enzymatic polymerization. *Polymers* **2012**, *4*, 116-133, https://doi.org/10.3390/polym4010116.
20. Kadokawa, J. Architecture of amylose supramolecules in form of inclusion complexes by phosphorylase-catalyzed enzymatic polymerization. *Biomolecules* **2013**, *3*, 369-385, https://dx.doi.org/10.3390%2Fbiom3030369.
21. Kadokawa, J. Chemoenzymatic synthesis of functional amylosic materials. *Pure Appl. Chem.* **2014**, *86*, 701-709, https://doi.org/10.1515/pac-2013-1116.
22. Kadokawa, J.; Shoji, T.; Yamamoto, K. Preparation of supramolecular network materials by means of amylose helical assemblies. *Polymer* **2018**, *140*, 73-79, https://doi.org/10.1016/j.polymer.2018.02.023.
23. Orio, S.; Shoji, T.; Yamamoto, K.; Kadokawa, J. Difference in macroscopic morphologies of amylosic supramolecular networks depending on guest polymers in vine-twining polymerization. *Polymers* **2018**, *10*, https://doi.org/10.3390/polym10111277.
24. Kadokawa, J.; Orio, S.; Yamamoto, K. Formation of microparticles from amylose-grafted poly(γ-glutamic acid) networks obtained by thermostable phosphorylase-catalyzed enzymatic polymerization. *RSC Adv.* **2019**, *9*, 16176-16182, https://doi.org/10.1039/c9ra02999k.
25. Kadokawa, J.; Tanaka, K.; Yamamoto, K. Enzymatic preparation of supramolecular networks composed of amylosic inclusion complexes with grafted guest polymers. *J. Electrochem. Soc.* **2019**, *166*, B3171-B3175, https://doi.org/10.1149/2.0311909jes.
26. Kadokawa, J.; Shoji, T.; Yamamoto, K. Preparation of amylose-carboxymethyl cellulose conjugated supramolecular networks by phosphorylase-catalyzed enzymatic polymerization. *Catalysts* **2019**, *9*, https://doi.org/10.3390/catal9030211.
27. Ziegast, G.; Pfannemuller, B. Phosphorolytic syntheses with di-functional, oligo-functional and multifunctional primers. *Carbohydr. Res.* **1987**, *160*, 185-204, https://doi.org/10.1016/0008-6215(87)80311-7.
28. Fujii, K.; Takata, H.; Yanase, M.; Terada, Y.; Ohdan, K.; Takaha, T.; Okada, S.; Kuriki, T. Bioengineering and application of novel glucose polymers. *Biocatal. Biotransform.* **2003**, *21*, 167-172, https://doi.org/10.1080/1024240310001614379.
29. Seibel, J.; Jordening, H.J.; Buchholz, K. Glycosylation with activated sugars using glycosyltransferases and transglycosidases. *Biocatal. Biotransform.* **2006**, *24*, 311-342, https://doi.org/10.1080/10242420600986811.
30. Yanase, M.; Takaha, T.; Kuriki, T. a-Glucan phosphorylase and its use in carbohydrate engineering. *J. Sci. Food Agric.* **2006**, *86*, 1631-1635, https://doi.org/10.1002/Jsfa.2513.
31. Kadokawa, J. α-Glucan phosphorylase-catalyzed enzymatic reactions using analog substrates to synthesize non-natural oligo-and polysaccharides. *Catalysts* **2018**, *8*, https://doi.org/10.3390/catal8100473.
32. Kadokawa, J.I. Enzymatic synthesis of functional amylosic materials and amylose analog polysaccharides. *Methods in Enzymology* **2019**, *626*, pp 189-213, https://doi.org/10.1016/bs.mie.2019.06.009.
33. Kadokawa, J. α-glucan phosphorylase-catalyzed enzymatic reactions to precisely synthesize non-natural polysaccharides. *ACS Symposium Series* **2020,** *1373*, 31-46, https://doi.org/10.1021/bk-2020-1373.ch002.
34. Awad, F.N. Glycoside phosphorylases for carbohydrate synthesis: An insight into the diversity and potentiality. *Biocatal. Agric. Biotechnol.* **2021**, *31*, https://doi.org/10.1016/j.bcab.2020.101886.
35. Kadokawa, J.; Kaneko, Y.; Tagaya, H.; Chiba, K. Synthesis of an amylose-polymer inclusion complex by enzymatic polymerization of glucose 1-phosphate catalyzed by phosphorylase enzyme in the presence of polyTHF: A new method for synthesis of polymer-polymer inclusion complexes. *Chem. Commun.* **2001**, 449-450, https://doi.org/10.1039/B008180i.
36. Kadokawa, J.; Kaneko, Y.; Nakaya, A.; Tagaya, H. Formation of an amylose-polyester inclusion complex by means of phosphorylase-catalyzed enzymatic polymerization of a-D-glucose 1-phosphate monomer in

the presence of poly(e-caprolactone). *Macromolecules* **2001**, *34*, 6536-6538, https://doi.org/10.1021/Ma010606n.
37. Kadokawa, J.; Kaneko, Y.; Nagase, S.; Takahashi, T.; Tagaya, H. Vine-twining polymerization: Amylose twines around polyethers to form amylose - Polyether inclusion complexes. *Chem. Eur. J.* **2002**, *8*, 3321-3326, https://doi.org/10.1002/1521-3765(20020802)8:15<3321::Aid-Chem3321>3.0.Co;2-E.
38. Kadokawa, J.; Nakaya, A.; Kaneko, Y.; Tagaya, H. Preparation of inclusion complexes between amylose and ester-containing polymers by means of vine-twining polymerization. *Macromol. Chem. Phys.* **2003**, *204*, 1451-1457, https://doi.org/10.1002/macp.200350004.
39. Kaneko, Y.; Beppu, K.; Kadokawa, J. Preparation of amylose/polycarbonate inclusion complexes by means of vine-twining polymerization. *Macromol. Chem. Phys.* **2008**, *209*, 1037-1042, https://doi.org/10.1002/macp.200800006.
40. Kaneko, Y.; Ueno, K.; Yui, T.; Nakahara, K.; Kadokawa, J. Amylose's recognition of chirality in polylactides on formation of inclusion complexes in vine-twining polymerization. *Macromol Biosci* **2011**, *11*, 1407-1415, https://doi.org/10.1002/mabi.201100133.
41. Kadokawa, J.; Yano, K.; Orio, S.; Yamamoto, K. Formation of supramolecular soft materials from amylosic inclusion complexes with designed guest polymers obtained by vine-twining polymerization. *ACS Omega* **2019**, *4*, 6331-6338, https://doi.org/10.1021/acsomega.9b00238.
42. Verbraeken, B.; Monnery, B.D.; Lava, K.; Hoogenboom, R. The chemistry of poly(2-oxazoline)s. *Eur. Polym. J.* **2017**, *88*, 451-469, https://doi.org/10.1016/j.eurpolymj.2016.11.016.
43. Glassner, M.; Vergaelen, M.; Hoogenboom, R. Poly(2-oxazoline)s: A comprehensive overview of polymer structures and their physical properties. *Polym. Int.* **2018**, *67*, 32-45, https://doi.org/10.1002/pi.5457.
44. Lorson, T.; Lübtow, M.M.; Wegener, E.; Haider, M.S.; Borova, S.; Nahm, D.; Jordan, R.; Sokolski-Papkov, M.; Kabanov, A.V.; Luxenhofer, R. Poly(2-oxazoline)s based biomaterials: A comprehensive and critical update. *Biomaterials* **2018**, *178*, 204-280, https://doi.org/10.1016/j.biomaterials.2018.05.022.
45. Viegas, T.X.; Fang, Z.; Yoon, K.; Weimer, R.; Dizman, B. Poly(oxazolines). In: *Engineering of Biomaterials for Drug Delivery Systems: Beyond Polyethylene Glycol*. **2018**; pp 173-198, https://doi.org/10.1016/B978-0-08-101750-0.00006-4.
46. Dargaville, T.R.; Park, J.-R.; Hoogenboom, R. Poly(2-oxazoline) hydrogels: State-of-the-art and emerging applications. *Macromol. Biosci.* **2018**, *18*, https://doi.org/10.1002/mabi.201800070.
47. Sahn, M.; Weber, C.; Schubert, U.S. Poly(2-oxazoline)-containing triblock copolymers: Synthesis and applications. *Polym. Rev.* **2019**, *59*, 240-279, https://doi.org/10.1080/15583724.2018.1496930.
48. Trachsel, L.; Romio, M.; Ramakrishna, S.N.; Benetti, E.M. Fabrication of biopassive surfaces using poly(2-alkyl-2-oxazoline)s: Recent progresses and applications. *Adv. Mater. Interfaces* **2020**, *7*, https://doi.org/10.1002/admi.202000943.
49. Zahoranová, A.; Luxenhofer, R. Poly(2-oxazoline)- and poly(2-oxazine)-based self-assemblies, polyplexes, and drug nanoformulations—An update. *Adv. Healthcare Mater.* **2021**, https://doi.org/10.1002/adhm.202001382.
50. Hoogenboom, R. Poly(2-oxazoline)s: A polymer class with numerous potential applications. *Angew. Chem. Int. Ed.* **2009**, *48*, 7978-7994, https://doi.org/10.1002/anie.200901607.
51. Oleszko-Torbus, N.; Utrata-Wesołek, A.; Bochenek, M.; Lipowska-Kur, D.; Dworak, A.; Wałach, W. Thermal and crystalline properties of poly(2-oxazoline)s. *Polym. Chem.* **2019**, *11*, 15-33, https://doi.org/10.1039/c9py01316d.
52. Witte, H.; Seeliger, W. Cyclische imidsäureester aus nitrilen und aminoalkoholen. *Liebigs Ann. Chem.* **1974**, *1974*, 996-1009, https://doi.org/10.1002/jlac.197419740615.
53. Smith, S.; Hubin, A.J. The preparation and chemistry of dicationically active polymers of tetrahydrofuran. *J. Macromol. Sci., Part A, Chem.* **1973**, *7*, 1399-1413, https://doi.org/10.1080/10601327308060509.
54. Bhuiyan, S.H.; Rus'd, A.A.; Kitaoka, M.; Hayashi, K. Characterization of a hyperthermostable glycogen phosphorylase from *Aquifex aeolicus* expressed in *Escherichia coli*. *J. Mol. Catal. B, Enzym.* **2003**, *22*, 173-180, https://doi.org/10.1016/s1381-1177(03)00029-8.
55. Yanase, M.; Takata, H.; Fujii, K.; Takaha, T.; Kuriki, T. Cumulative effect of amino acid replacements results in enhanced thermostability of potato type L a-glucan phosphorylase. *Appl. Environ. Microbiol.* **2005**, *71*, 5433-5439, https://doi.org/10.1128/Aem.71.9.5433-5439.2005.
56. Kobayashi, S.; Uyama, H.; Kimura, S. Enzymatic polymerization. *Chem. Rev.* **2001**, *101*, 3793-3818, https://doi.org/10.1021/cr990121l.
57. Yamashita, Y. Single crystals of amylose V complexes. *J. Polym. Sci. Part A* **1965**, *3*, 3251-3260, https://doi.org/10.1002/pol.1965.100030919.
58. Obiro, W.C.; Ray, S.S.; Emmambux, M.N. V-Amylose structural characteristics, methods of preparation, significance, and potential applications. *Food Rev. Int.* **2012**, *28*, 412-438, https://doi.org/10.1080/87559129.2012.660718.